Journal of Saudi Chemical Society (2023) **27**, 101622

King Saud University

Journal of Saudi Chemical Society

www.ksu.edu.sa
www.sciencedirect.com

ORIGINAL ARTICLE

Synthesis, characterization, biological applications, and molecular docking studies of amino-phenol-derived mixed-ligand complexes with Fe(III), Cr(III), and La(III) ions

Saud I. Al-Resayes [a], Fatima Y. Laria [b], Miloud M. Miloud [c], Marei M. El-ajaily [b,*], Najla M. El-Barasi [d], Ashish K. Sarangi [e], Sarika Verma [f,g], Mohammad Azam [a,*], Veronique Seidel [h], Ranjan K. Mohapatra [i,*]

[a] *Department of Chemistry, College of Science, King Saud University, PO BOX 2455, Riyadh 11451, Saudi Arabia*
[b] *Chemistry Department, Faculty of Science, Benghazi University, Benghazi, Libya*
[c] *Botany Department, Faculty of Science, Benghazi University-Al-abiar branch, Benghazi, Libya*
[d] *Chemistry Department, Faculty of Science, Benghazi University-Tawkra branch, Benghazi, Libya*
[e] *Department of Chemistry, School of Applied Sciences, Centurion University of Technology and Management, Odisha, India*
[f] *Council of Scientific and Industrial Research-Advanced Materials and Processes Research Institute (AMPRI), Hoshangabad Road, Bhopal-462026, MP, India*
[g] *AcSIR-Advanced Materials and Processes Research Institute (AMPRI), Hoshangabad Road, Bhopal 462026, MP, India*
[h] *Natural Products Research Laboratory, Strathclyde Institute of Pharmacy and Biomedical Sciences, University of Strathclyde, Glasgow G4 0RE, UK*
[i] *Department of Chemistry, Government College of Engineering, Keonjhar 758002, Odisha, India*

Received 9 May 2022; revised 19 February 2023; accepted 24 February 2023
Available online 15 March 2023

KEYWORDS

Schiff base ligand;
Mixed-ligand complexes;
Antibacterial activity;
Anti-cancer activity;
Molecular docking study;
QSAR study

Abstract A new series of Fe(III), Cr(III), and La(III) mixed-ligand complexes, resulting from the interaction of 2-aminophenol with 2-hydroxy acetophenone (HL_1) as primary ligand and L- histidine (L_2) as a secondary ligand, has been investigated using various physicochemical studies such as elemental analyses, molar conductivity, magnetic moment, infrared, UV/Vis, ^{1}H NMR, and mass spectroscopic techniques. The microanalytical results indicate that the mixed ligand complexes were designed in a 1:1:1 M ratio. The electronic spectral data indicated that all the synthesized complexes have an octahedral structure. The disc diffusion assay was used to determine the disc inhibition zone (IZ, mm) and minimum inhibitory concentration (MIC, g/mL) of the investigated compounds against the growth of the pathogenic bacterial strains *S. aureus*, *E. faecalis*, *P. aeruginosa*, *Klebsiella sp.*, and *E. coli*. The MTT test was used to determine the cytotoxicity of these reported compounds against the human hepatocellular liver cancer (HEPG-2) cell lines. The molecular docking study for the compounds against the EGFR tyrosine kinase receptor (PDB code: 1 M17) was conducted to

* Corresponding authors.
E-mail addresses: melajaily@gmail.com (M.M. El-ajaily), azam_res@yahoo.com, mhashim@ksu.edu.sa (M. Azam), ranjank_mohapatra@yahoo.com (R.K. Mohapatra).

https://doi.org/10.1016/j.jscs.2023.101622

examine the interactions in protein–ligand complexes. Furthermore, the biological activity of the ligand was investigated using quantitative structure–activity relationship studies (QSAR).

1. Introduction

Schiff bases have long been recognized as useful ligands in coordination chemistry because of their significant roles as intermediates in many biological enzymatic reactions, and as catalysts in chemistry [1-3]. Reports reveal that the demonstration of biological applications is due to the lone pair of electrons on the sp2 hybridized orbital of imine nitrogen, which is responsible for a wide range of antimicrobial, anticancer, herbicidal, and clinical properties [3-6]. Schiff bases are widely investigated because of their adaptability, selectivity, and sensitivity to the metal ions, structural resemblances with natural biological constituents, and an imine linkage (–CH = N-) to explain the mechanism of transformation and resemination reaction in biological systems [5]. In addition to their attractive physical properties, Schiff bases are best suited to coordinating with a range of transition metal ions due to the hard nitrogen or oxygen atoms and the soft sulfur atoms in their backbone, resulting in gorgeously colored and stable metal complexes with an intriguing chemical and physical behavior [7,8]. Complexes derived from Schiff bases have received enormous interest from researchers worldwide over the years due to their remarkable contributions in the area of material sciences, catalysis, magnetism, and a variety of industrial and biological reactions [7-9]. Amino acid-based Schiff base complexes have been identified as a new class of pharmacologically active compounds in biological systems, as well as being capable of a variety of catalytic applications [10,11].

Mixed-ligand complexes with nitrogen and oxygen-donor have gained significant attention because of their exceptional stability [12], and efficacy as metal systems for metal-protein complexes such as metalloenzymes [13]. Furthermore, they have been used in protein molecular cartography for surface relief analyses, biological redox centers, protein collection and purification, the food and dye industry, as well as potential pharmacological agents like antimicrobial, anti-inflammatory, anti-hypertensive, antiarthritic, antiviral, and anticancer agent [14-16]. In a mixed-ligand complex, ligands can help identify biological target areas such as DNA, enzymes, and protein receptors by determining not only the reactivity of the metals but also the nature of secondary coordination sphere connections. [17,18]. It is well known that amino acids can chelate metal ions due to the negative charge of their –NH2 and –COO- groups, which bind with the metal ion, respectively. Furthermore, the interaction of metal ions with amino acids stabilizes the protein structure and results in enzymatic activity [19,20]. There are several reports in the literature that mixed-ligand complexes with amino acids as secondary ligands play an important role as models for enzyme metal ion substrate complexes [21]. Histidine, an essential amino acid, is the most common ligand in the active center of zinc-containing enzymes [22]. Therefore, considering the importance of amino-acid, we are herein interested in the synthesis and Physico-chemical studies of mixed ligand complexes of Fe(III), Cr(III), and La(III) ions with HL_1 as the primary ligand, and L_2 as a secondary ligand. The investigated compounds were tested for antimicrobial and anticancer activity. Additionally, molecular docking studies have been carried out.

2. Experimental

2.1. Material and methods

All materials employed such as aminophenol, 2-hydroxy acetophenone, L-histidine, DMF, DMSO, NaOH, methanol, and metal salts were of pure grade. The CHN analysis of the prepared complexes was carried out using the 2400-CHN elemental analyzer. Molar conductance was measured in dimethylformamide using a CMD-650 digital conductivity meter. An IFS-25 DPUS/I spectrometer was used to collect the IR spectra. The ^{1}HNMR spectra were obtained in d_6-DMSO on a Varian Gemini 200 MHz spectrometer with TMS as an internal standard. Spectra of UV/Vis and mass were obtained using spectrophotometers from Perkin-Elmer lambda-365 and Shimadzu QP-2010 Plus, respectively.

2.2. Synthesis of Schiff base ligand, HL_1

2-aminophenol (1.09 g, 0.01 mol) and 2-hydroxyacetophenone (1.39 g, 0.01 mol) were mixed in a methanolic solution in the presence of a catalytic quantity of acid and refluxed for 3 h to result in a precipitate, which was filtered, air dried, and then recrystallized with the methanol-dichloromethane mixture to obtain pure crystalline compound (Scheme 1).

2.3. Synthesis of the mixed-ligand complexes

The mixed ligand complexes with Fe(III), La(III), and Cr(III) ions were made by mixing (0.01 mol, 2.28 g) of HL_1 in methanol with 0.01 mol of the required metal salts ($FeCl_3{\cdot}6H_2O$, $CrCl_3{\cdot}6H_2O$, $La(NO_3)_3{\cdot}6H_2O$) (Scheme-1). To keep the pH at 8, a few drops of NaOH solution were gently added. After three hours of stirring and refluxing, a solution of histidine (L_2) (0.01 mol, 1.55 g) in 25 cm^3 of distilled water was added to the reaction mixture, which was additionally refluxed for 3 more hours. The precipitate was separated and rinsed multiple times with ethanol until it was clear, then dried in a desiccator with anhydrous $CaCl_2$.

2.4. In vitro antibacterial activity

The antibacterial activity of these compounds was tested using an agar well diffusion assay against *S. aureus, E. faecalis, P. aeruginosa, Klebsiella* sp., and *E. coli*. We also observed the antibacterial activity of metal salts and compared the results. The bacterial species is used at a concentration of 100 mg/

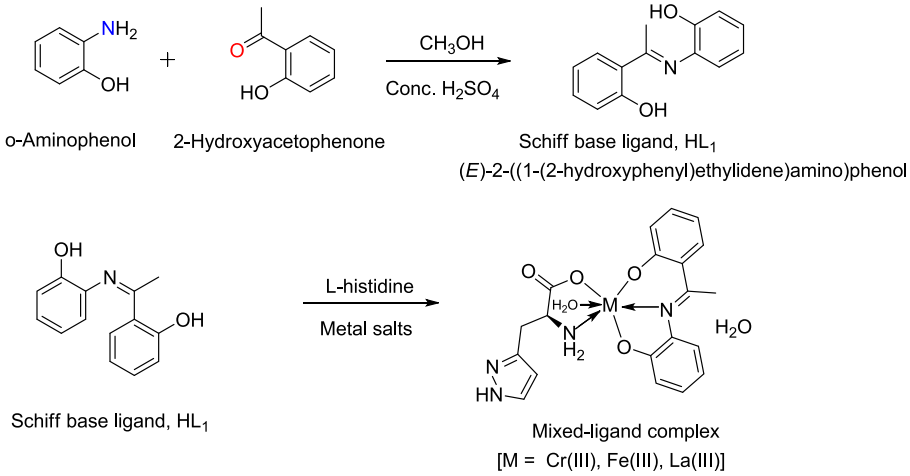

Scheme 1 Synthesis of the Schiff base ligand and its mixed-ligand complexes.

mL. DMF is used as a negative control, while tetracycline is used as a positive control.

2.5. Determination of cytotoxicity by MTT assay

The MTT test was used to determine the cytotoxicity of the compounds under investigation. Human hepatocellular liver cancer (HEPG-2) cell lines were acquired under liquid nitrogen (-180 °C) and kept alive through successive sub-culturing at the National Cancer Institute (NCI), Cairo University, Egypt. To generate a full monolayer sheet, 1 X 10^5 cells/mL (100 ul/well) were seeded into a 96-well tissue culture plate and cultured at 37 ℃ for 24 h. Once the cells were confluent, the growth media was separated from the 96-well microtiter plates, and a wash medium was used to wash the monolayer of cells twice. A maintenance medium in RPMI medium containing 2% serum was prepared by diluting the tested compounds two-fold (maintenance medium). Three wells acted as controls, receiving just maintenance medium, while each well was evaluated with 0.1 mL of each dilution. Physical evidence of toxicity, such as loss of monolayer, rounding, shrinkage, or granulation of cells, was assessed by visually inspecting the plate after 37 °C incubation. Five milligrams per milliliter of PBS was used to make the MTT solution (BIO BASIC CANADA INC). A 5-minute shaking at 150 rpm was employed to mix the MTT into the medium for each well-received 20ul of MTT solution. To digest the MTT, incubate it for 1–5 h at 37 °C with 5% CO2. Remove the medium from the room. If necessary, wipe the plate clean with paper towels and resuspend the formazan in 200ul DMSO (MTT metabolic product). Shake the formazan and solvent together thoroughly for 5 min at 150 rpm. An Optical density was measured at 560 nm, with 620 nm used to subtract ambient light. The ratio of cells to optical density should be maintained.

3. Results and discussion

Elemental analysis of the ligand and its complexes is shown in Table 1. The experimental findings are in good agreement, demonstrating the synthesis of complexes [M:L:L] in an equimolar ratio. The molar conductivity data of the complexes [11] demonstrated their non-electrolytic character. The percentage of water lost in the synthesized compounds [Cr-complex (7.65%), Fe-complex (7.61%), and La-complex (6.45%) were determined in the temperature range of 70–180 °C] by utilizing thermogravimetric methods.

3.1. Infrared spectra

Table 2 shows the IR data of the mixed ligand complexes. The infrared spectrum of the primary ligand, HL_1 reveals a band at 1609 cm^{-1} corresponding to the C = N vibration [8,24]. The –OH band appears at 3410 cm^{-1} [8]. The band at 1440 cm^{-1} corresponds to the bending vibration of the NH_2 group. However, these bands shifted (lower) in the spectra of complexes, suggesting the participation of azomethine (C = N) nitrogen, phenolic (–OH) oxygen, and –COOH and $–NH_2$ group of histidine in coordination [8,24,25]. The absorption bands of OCO– asymmetric valence vibrations (1605–1580 cm-1) and symmetric OCO– vibrations (1442, 1381 cm-1) were also observed in the studied mixed-ligand complexes [25]. Furthermore, the vibrations due to the –COO group in the studied complexes showed peaks at 748, 609, and 540 cm^{-1}, corresponding to its wagging, bending, and rocking respectively [25]. However, the appearance of the band in the 3450–3465 cm^{-1} range is attributed to the presence of water molecules [26]. The spectra of mixed-ligand complexes revealed bands at 3100–3130 cm^{-1} assigned to –NH (primary amine) stretching vibration [27] [Supplementary Information Figures S1-S4].

3.2. Mass spectra

The mass spectrometry method is often used to determine the composition of a sample by creating a mass spectrum that depicts the masses of sample components, but it may also be used to identify unknown chemicals based on their mass or fragments [28]. A molecular ion [M +] peak is observed at m/z = 228 [Fig. 1], which corresponds to its molecular weight, $C_{14}H_{14}NO_2$. However, the shatter peaks at m/z 212, 134, 109, and 80 are caused by the splitting of $[C_{14}H_{13}NO]^+$, $[C_8H_8NO]$, $[C_7H_8O]^+$, and $[C_6H_8]$ [Scheme 2].

Table 1 Physico-chemical properties of the compounds.

Compounds	M. Wt.	Yield (%)	Mp (℃)	Color	C% (Cal.) Found	H% (Cal.) Found	N% (Cal.) Found	M% (Cal.) Found	μ (B. M)
HL_1	227	88	> 250	Yellow	(73.68) 73.50	(5.70) 5.54	(6.14) 6.04	–	–
$[Cr(L_1)(L_2)(H_2O)]H_2O$	466	72.5	> 250	Seaweed	(51.28) 51.07	(4.49) 4.24	(11.97) 11.60	(11.16) 11.05	4.01
$[FeL_1(L_2)(H_2O)]H_2O$	470	73.4	> 250	Hickory	(50.85) 50.66	(4.45) 4.24	(11.86) 11.64	(11.91) 11.84	5.85
$[LaL_1(L_2)(H_2O)]H_2O$	553	69.7	> 250	Wine	(43.24) 43.15	(3.78) 3.57	(10.09) 9.95	(25.13) 24.97	0.00

Table 2 IR (cm^{-1}) and UV/Vis data of the compounds.

Compounds	ν(COO⁻)	ν (H_2O)	ν(C = N)	ν (NH)	ν (M–O)	ν (M–N)	nm (cm^{-1})
HL_1	–	3875	1705	–	–	–	289 (34602)-310 (32258)
L_2	–	–	–	–	–	–	215 (46511)
$[Cr(L_1)(L_2)(H_2O)]H_2O$	1597, 1442, 748, 609, 540	3418	1697	3240	655	480	299 (33444)-429 (23310)-504 (19841)
$[Fe(L_1)(L_2)(H_2O)]H_2O$	1604, 748, 621, 540	3464	1686	3240	670	474	310 (32258)-430 (23255)
$[La(L_1)(L_2)(H_2O)]H_2O$	1581, 1381, 743, 609, 540	3541	1682	3240	650	495	303 (33003)-384 (26042)

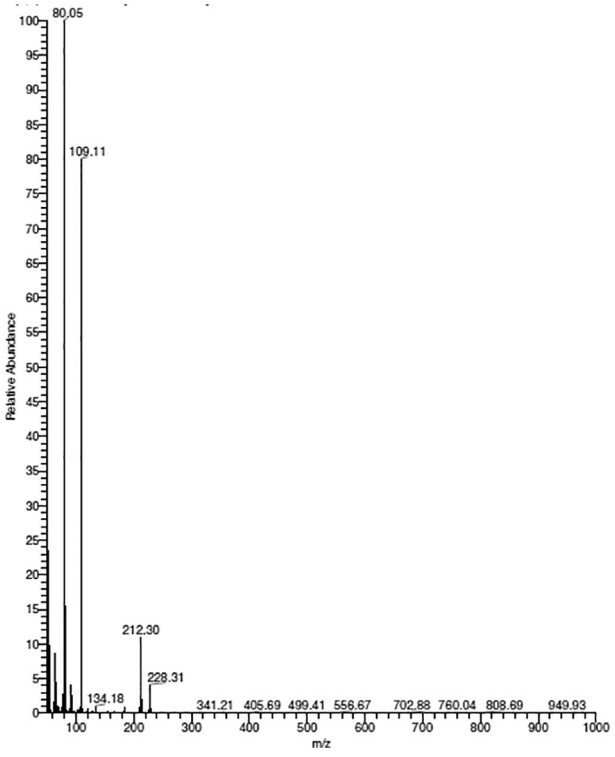

Fig. 1 Mass spectrum of the ligand, HL_1.

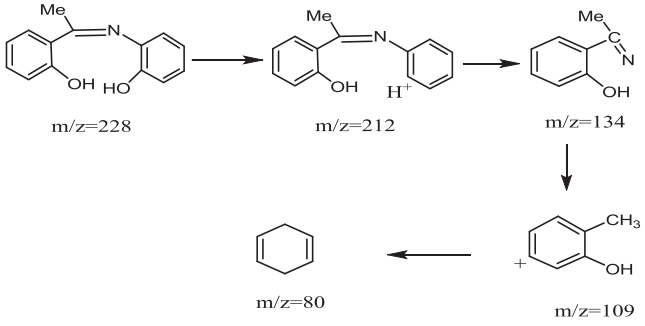

Scheme 2 Mass spectral fragmentation of the ligand, HL_1.

3.3. Electronic spectra and magnetic moments

Electronic spectra of the ligand, HL_1, and its mixed-ligand complexes [Supplementary Information Figure S5] were recorded in 10^{-3} M DMF at room temperature and their assignments are listed in Table 2. The ligand HL_1 shows two bands at 289 nm (34602 cm^{-1}) and 310 nm (32258 cm^{-1}), which correspond to π-π* (phenyl ring) and n-π* transitions, respectively [6,29]. The electronic spectrum of the Cr-mixed-ligand complex exhibits three bands at 299 nm (33444 cm^{-1}), 429 nm (23310 cm^{-1}) and 504 nm (19841 cm^{-1}) due to intra-ligand charge transfer, $^4A_{2g}(F)\rightarrow{}^4T_{1g}(F)$ and $^4A_{2g}(F)\rightarrow{}^4T_{2g}(F)$, respectively. Furthermore, a magnetic moment at 4.01B. M. of the complex is equivalent to the existence of three unpaired electrons at the spin-only value, implying that chromium in the complex has an octahedral geometry [29,30]. The UV/Vis spectra of Fe-mixed-complex exhibit two bands at 310 nm (32258 cm^{-1}) and 430 nm (23255 cm^{-1}) that correspond to $^6A_{1g}\rightarrow{}^4E_g(G)$, $^6A1g\rightarrow{}^4T_{2g}(D)$,$^6A_{1g}\rightarrow{}^4E_g(D)$ transitions, and metal to ligand charge transfer transitions, respectively. Furthermore, the magnetic moment value for the Fe-mixed-ligand complex being 5.85 BM indicates that Fe(III) exists in the octahedral environment for the complex [29,30]. The electronic spectrum of the La-mixed-ligand com-

plex exhibits two bands at 303 nm (33003 cm^{-1}) and 384 nm (26042 cm^{-1}) ascribed to π-π*, n-π* transition, and LMCT, respectively.

3.4. ^{1}H NMR spectra

The resonance signal due to methyl protons was found at 2.25–2.60 ppm in the ^{1}H NMR spectra, whereas the multiplet due to aromatic proton was observed at 6.38–7.95 ppm, validating the synthesis of the primary ligand, HL_1 (Fig. 2) [Supplementary Information Table S1].

3.5. Antibacterial activity

The antibacterial efficacy of the produced compounds against pathogens is shown in Table 3. All metal salts and 2-aminophenol showed significant antibacterial activity when compared to the Schiff base ligand (HL_1) [Fig. 3], whereas Histidine (L_2) and the synthesized mixed-ligand metal complexes did not affect pathogens. Tetracycline was most effective against three bacteria, *S. aureus*, *E. faecalis*, and *P. aeruginosa*, whereas it was least effective against *Klebsiella* sp. and *E. coli* [Fig. 3]. The MIC values of the most effective compounds (2-aminophenol, $CrCl_3{\cdot}6H_2O$, and $La(NO_3)_3{\cdot}6H_2O$ were also determined. The effective compounds' concentration effects were reported in (Table-4). The inhibitory effect of 2-aminophenol began at 3.1 mg/mL against *S. aureus* and *Klebsiella* sp. with inhibition zones of 8 mm and 7 mm, progressed to 6.2 mg/mL with an inhibition zone of 9 mm against *E. faecalis*, and finally reached 12.5 mg/mL with inhibition zones of 9 mm and 7 mm against *P. aeruginosa* and *E. coli*. The inhibitory effect of $CrCl_3{\cdot}6H_2O$ began at 6.2 mg/mL with inhibition zones of 7–8 mm against all tested bacterial species, whereas $La(NO_3)_3{\cdot}6H_2O$ inhibited bacterial growth at 12.5 mg/mL with inhibition zones of 9, 10, 10, and 8 mm against *S. aureus, P. aeruginosa, Klebsiella* sp., and *E. coli*, except *E. faecalis*, which was highly sensitive and had a MIC of 6.2 mg/mL. $CrCl_3{\cdot}6H_2O$ inhibited bacterial growth at 6.2 mg/mL with inhibition zones of 7–8 mm against all tested bacterial species, whereas $La(NO_3)_3{\cdot}6H_2O$ inhibited bacterial growth at 12.5 mg/mL with inhibition zones of 9, 10, 10, and 8 mm against *S. aureus, P. aeruginosa, Klebsiella* sp., and *E.coli*, except *E. faecal*, which was extremely susceptible with a MIC of 6.2 mg/mL [Supplementary Information Figures S6-S13].

3.6. Anticancer activity

To evaluate cell proliferation, the in-vitro inhibitory efficacy of the investigated compounds was performed against the HEPG-2 cell line together with the standard anticancer drug doxorubicin. The cytotoxicity of the primary ligand, HL_1, and its metal complexes was tested at different concentrations (0–1000 μgmL^{-1}). Cell proliferation was reduced after incubation

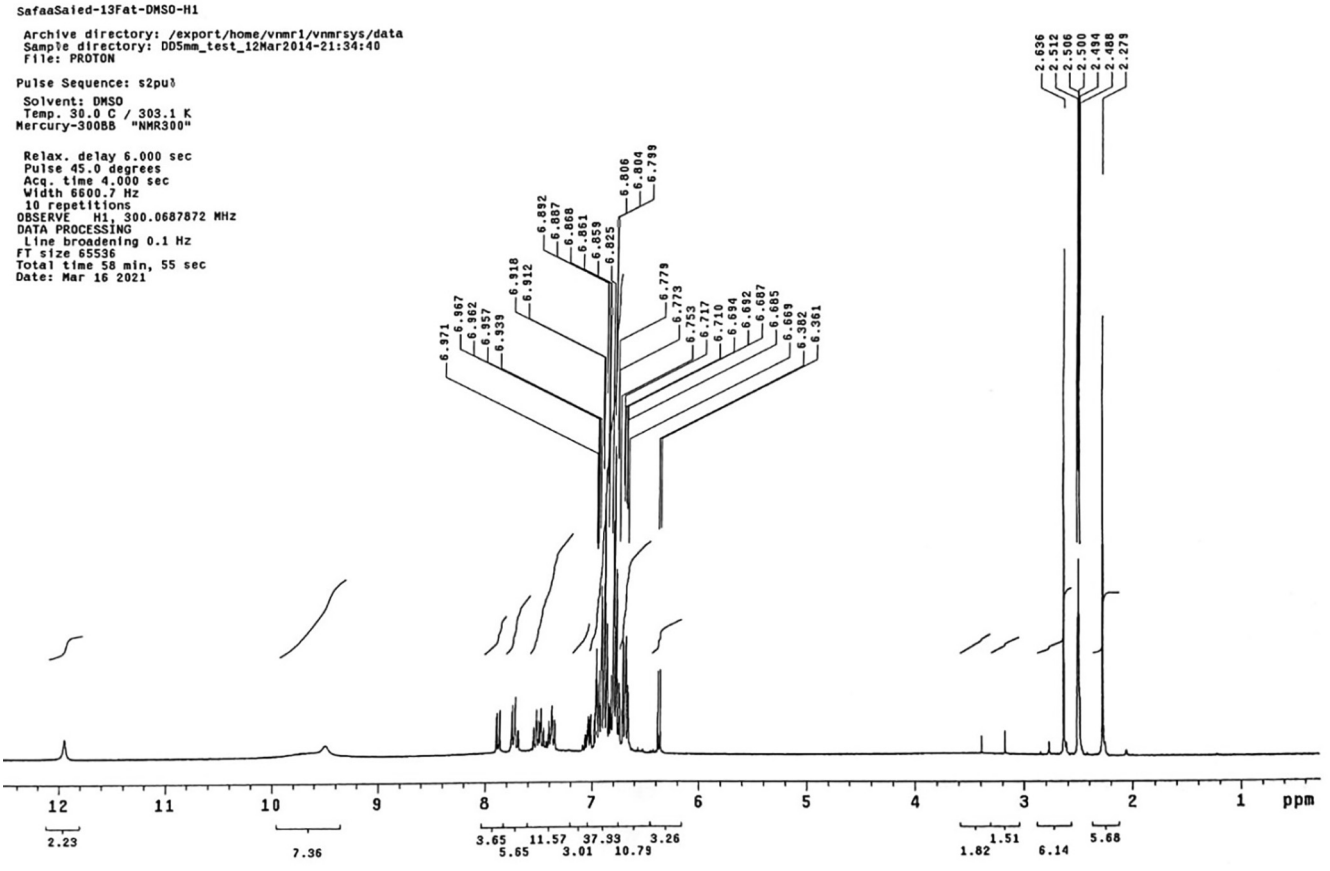

Fig. 2 ^{1}HNMR spectrum of the ligand, HL_1.

Table 3 Results of antibacterial activity of selected compounds against bacterial species.

No.	Compounds	Inhibition Zone measured in millimeter				
		Concentration 100 mg/ml				
		Gram (+ve) pathogenic bacteria		Gram (-ve) pathogenic bacteria		
		S. aureus	*E. faecalis*	*P. aeruginosa*	*Klebsiella* sp.	*E. coli*
1	Schiff base (L_1)	11	10	10	12	8
2	Histidine (L_2)	R	R	R	R	R
3	2-aminophenol	13	13	13	16	12
4	Cr - complex	R	R	R	R	R
5	La - complex	R	R	R	R	R
6	Fe -complex	R	R	R	R	R
7	Cr-salt	14	14	13	14	14
8	La-salt	14	14	13	13	14
9	Fe-salt	11	12	10	12	12
10	C^+ Tetracycline	17	15	14	12	12
11	C^- DMF	R	R	R	R	R

C^+**:** Positive control**,** C^-**:** Negative control, **R:** Resistant.

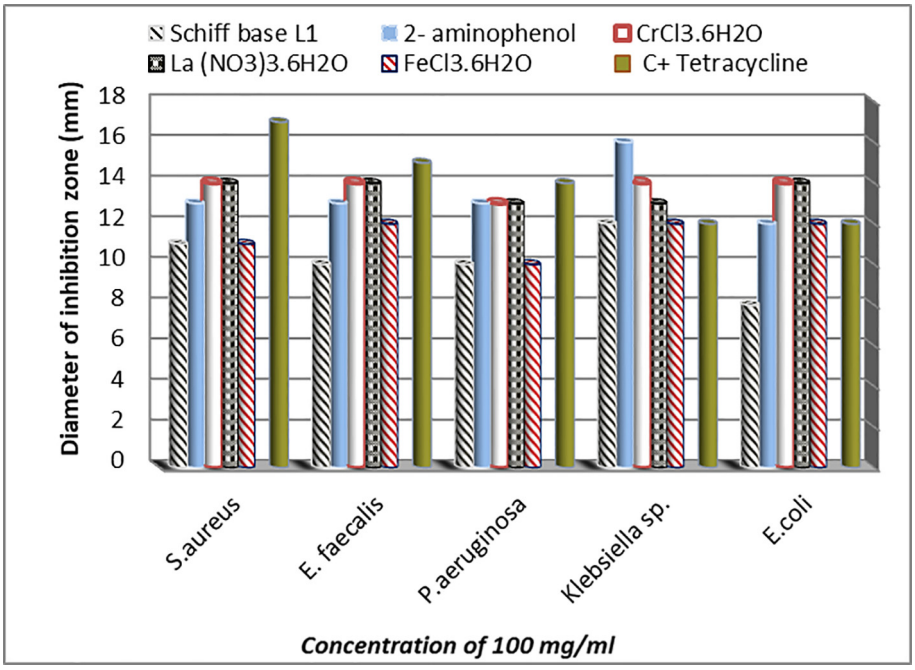

Fig. 3 Effect of compounds and antibiotics against bacterial species.

with complexes. The mixed-ligand complexes have stronger cytotoxic activity than the free ligand. Fig. 4 depicts the surviving fraction of the compounds against HepG2 cell lines. The IC_{50} values of the complexes under study were determined and compared to those of doxorubicin, a standard anticancer medication [31,32]. When compared to the standard doxorubicin, the obtained data revealed that all of the tested compounds have weak anticancer activity due to higher IC_{50} values [33].

3.7. Molecular docking study

The Molecular Operating Environment (MOE) 2009.10 application was utilized in molecular docking investigations [21]. The binding free energy of the inhibitor within the macromolecule was determined by docking tests. To confirm that

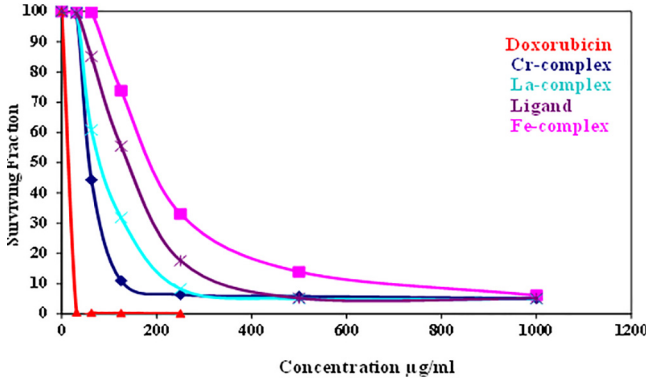

Fig. 4 The surviving fraction of compounds against HEPG2 liver cells.

Table 4 MIC of the most effective compounds against pathogenic bacteria.

No.	Compounds	The zone of inhibition is measured in millimeter					
		Concentrations (mg/mL)	Gram (+ve) bacteria		Gram (-ve) bacteria		
			S. aureus	*E. faecalis*	*P. aeruginosa*	*Klebsiella* sp.	*E. coli*
1	2-aminophenol	3.1	8	R	R	7	R
		6.2	11	9	R	13	R
		12.5	11	10	9	13	7
		25	12	11	10	14	8
		50	12	12	11	14	10
		100	13	13	14	16	12
2	$CrCl_3{\cdot}6H_2O$	3.1	R	R	R	R	R
		6.2	7	7	8	8	8
		12.5	8	9	10	9	9
		25	10	10	11	11	10
		50	10	12	12	12	11
		100	14	14	14	14	14
3	$La(NO_3)_3{\cdot}6H_2O$	3.1	R	R	R	R	R
		6.2	R	8	R	R	R
		12.5	9	10	10	10	8
		25	10	10	11	11	12
		50	12	12	12	11	12
		100	14	14	14	14	14

R: Resistant.

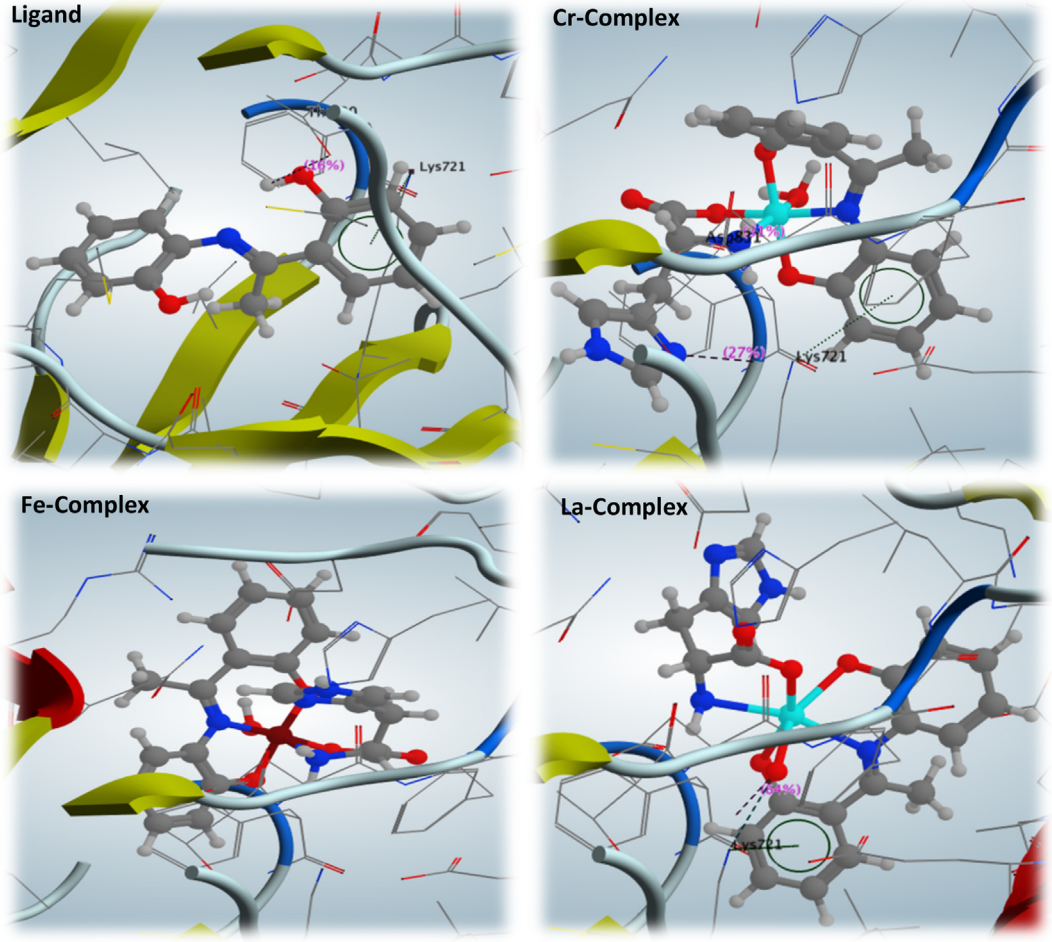

Fig. 5 3D Binding affinity of compounds against EGFR tyrosine kinase receptor (PDB Code: 1 M17).

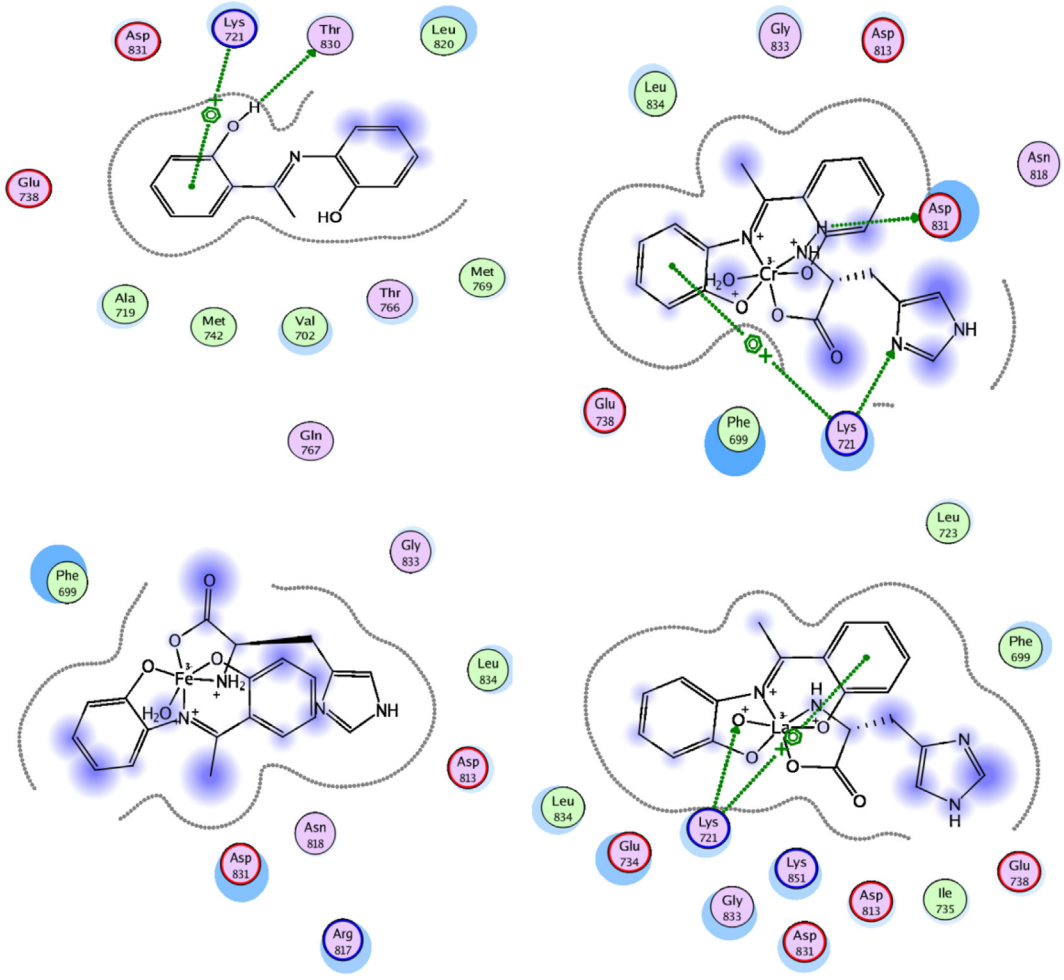

Fig. 6 2D Binding affinity of compounds against EGFR tyrosine kinase receptor (PDB Code: 1 M17).

Table 5 The binding affinity of the compounds against EGFR tyrosine kinase receptor (PDB Code: 1 M17).

Antitumor docking against PDB Code: 1 M17			
Compound	Scoring energy (RMSD)	Involved amino acids	Type of interaction
Schiff base	−4.60 (1.57)	Lys-721 and Thr-830	Arene-cation interaction and side chain acceptor
Cr - complex	−5.49 (1.77)	Lys-721and Asp-831 (-5.49) (1.77)	(Arene-cation interaction & Side chain acceptor) and side chain donor
Fe - complex	−4.61 (2.49)	–	Solvent contact
La - complex	−4.77 (2.45)	Lys-721	Arene-cation interaction and side chain donor

refined poses satisfy the specified conformations, the Dock scoring function in MOE software was employed, and the force-filed were improved. The top ten binding postures were directed to be evaluated to obtain the highest possible score. Auto-rotatable bonds were permitted, and the top ten binding poses were directed to be evaluated to acquire the highest possible score. The affinity of the compound utilized as a ligand for binding to the tyrosine kinase receptor (EGFR) was studied in this work. A three-dimensional model of the structures was created using MOE's molecular builder tool. Force-filled MMFF94X was used for energy minimization. The lowest energy conformation with the most advantageous geometry was found by optimizing with a gradient of 0.001 (see Table 4).

Table 6 QSAR calculations for the optimized ligand (HL_1).

Function	(Ligand) 2-(1-(2-hydroxyphenylimino) ethyl)phenol
Surface area (Approx) (Å^2)	302.77
Surface area (Grid) (Å^2)	429.04
Volume (Å^3)	708.96
Hydration energy (Kcal/mole)	−8.25
Log P	3.43
Refractivity (Å^3)	17.44
Polarizability (Å^3)	25.97
Mass (amu)	227.26
Total energy (kcal/mol)	−7.05733
Dipole Moment (Debye)	0.8898
Free energy (kcal/mol)	−7.05733
RMS Gradient (kcal/Å mol)	0.08464

The crystal structure of c-kit receptor protein-tyrosine kinase in the mixed-ligand complex was obtained using the Protein Data Bank (PDB) (PDB code: 1 M17). With the protonation of 3d application in MOE, partial charges and hydrogen atoms were added to the protein. The compounds investigated have intriguing interactions with the active site of amino acids of the EGFR tyrosine kinase receptor (Figs. 5 and 6). The most common amino acid residue involved in interactions is Lys-721. Table 5 shows the scoring energy, RMSD, type of amino acid residues, and type of interactions.

3.8. Quantitative Structure-Activity relationship studies (QSAR)

The goal of this investigation is to verify the properties, activities, and reactivities of the prepared complexes. All calculations were performed with the HyperChem Professional 8.0.3 application pack. The structure of the ligand, HL_1, is optimized using the (MM +) force field and semi-empirical PM3 methods. The log P value for the Schiff base ligand (HL_1 = 3.43) was calculated. The partition coefficient (log P) is critical in describing how the produced Schiff base ligand works biologically. The log P plays a key role in controlling the permeability of produced compounds through the cell membrane [34,35]. Other important physical characteristics, including surface area, volume, mass, total energy, free energy, refractivity, polarizability, hydration energy, and RMS gradient, are determined to infer the activity of HL_1 (Table 6).

3.9. ESP analysis

The software ArgusLab 4.0.1 was used to evaluate the ESP surface of HL1 [Fig. 7]. The ESP surface displayed the distribution of charges in a certain location. The surface of the ligand is littered with evident electrophilic attack sites. Negative areas over phenolic oxygen and azomethine nitrogen atoms were detected, as indicated by the red colour, and were involved in coordination [36]. The phenolic oxygen is linked to the central metal ion through deprotonation. The spectral analysis, however, confirms that there are no other sites for the electrophilic attack.

4. Conclusion

It can be concluded that the investigated mixed-ligand complexes have an octahedral structure and are formed in equimolar ratio. The complexes didn't exhibit significant antimicrobial activity in comparison to the Schiff base ligand, HL_1. In addition, the complexes also showed poor anticancer activity. However, the cytotoxic activity of the mixed-ligand complexes surpasses that of the free ligand. The molecular docking studies of the compounds against the EGFR tyrosine kinase receptor (PDB id: 1 M17) were discussed. The scoring energy and RMSD scores for the tested compounds were calculated. Moreover, the partition coefficient (log P) value for the Schiff base ligand (HL_1 = 3.43) was also calculated.

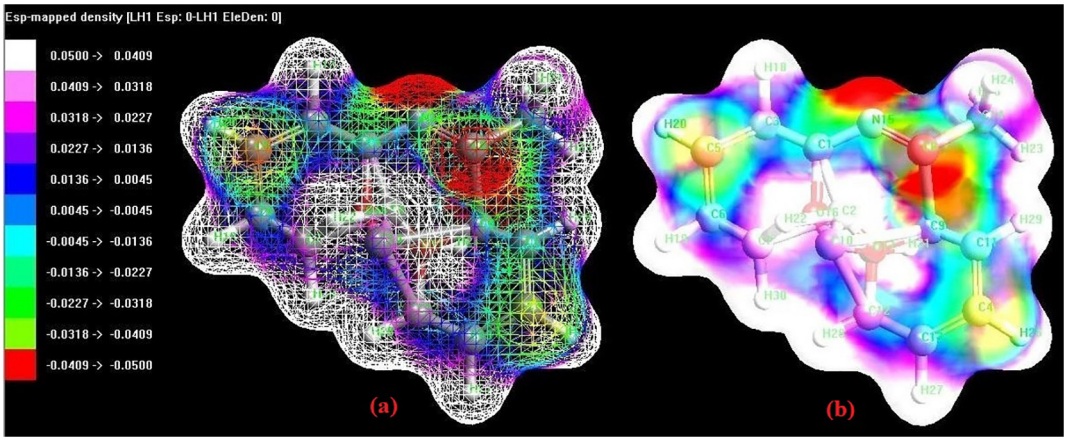

Fig. 7 The ESP surface of the ligand, HL_1.

Declaration of Competing Interest

The authors declare that they have no known competing financial interests or personal relationships that could have appeared to influence the work reported in this paper.

Acknowledgments

The authors acknowledge the financial support through the Researchers Supporting Project number (RSP2023R147), King Saud University, Riyadh, Saudi Arabia.

Appendix A. Supplementary data

Supplementary data to this article can be found online at https://doi.org/10.1016/j.jscs.2023.101622.

References

[1] E. Sinn, C.M. Harris, Coord. Chem. Rev. 4 (4) (1969) 391–422.
[2] S.K. Fathalla, H.A. El-Ghamry, M. Gaber, Inorg. Chem. Commun. 129 (2021) 108616.
[3] R.K. Mohapatra, P.K. Das, M.K. Pradhan, A.A. Maihub, M. M. El-ajaily, J. Iran Chem. Soc. 15 (2018) 2193–2227.
[4] M. Shakir, M. Azam, M.F. Ullah, S.M. Hadi, J. Photochem. Photobiol B. Biol. 104 (2011) 449–456.
[5] S. Patal, The Chemistry of Carbon Nitrogen Double Bond, Interscience Publishers Inc., New York, 1970.
[6] M. Shakir, M. Azam, Y. Azim, S. Parveen, A.U. Khan, Polyhedron 26 (2007) 5513–5518.
[7] M. Shakir, A. Abbasi, M. Azam, A.U. Khan, Spectrochim. Acta Part A 79 (5) (2011) 1866–1875.
[8] M. Azam, S. Dwivedi, S.I. Al-Resayes, S.F. Adil, M.S. Islam, A. Trzesowska-Kruszynska, R. Kruszynski, D.-U. Lee, J. Mole. Struct. 1130 (2017) 122–127.
[9] T.A. Fayed, M. Gaber, G.M. Abu El-Reash, M.M. El-Gamil, Appld. Organomet. Chem. 34 (9) (2020) e5800.
[10] M. Gaber, K. El-Baradie, N. El-Wakiel, S. Hafez, Appld. Organomet. Chem. 34 (2) (2020) e5348.
[11] G. Plesch, C. Friebel, O. Svajlenova, J. Kratsmar-Smogrovic, D. Mlynarcik, Inorg. Chim. Acta 151 (1988) 139–143.
[12] H. Sigel, B.P. Operschall, S.S. Massoud, B. Song, R. Griesser, Dalton Trans. 46 (2006) 5521–5529.
[13] J.R. Bocarsly, J.K. Barton, Inorg. Chem. 31 (13) (1992) 2827–2834.
[14] O. Farver, I. Pecht, Coord. Chem. Rev. 94 (1989) 17–45.
[15] J. Crowe, H. Döbeli, R. Gentz, E. Hochuli, D. Stüber, K. Henco, Methods Mol Biol. 31 (1994) 371–387.
[16] M. Azam, P.K. Sahoo, R.K. Mohapatra, M. Kumar, A. Ansari, I.S. Moon, A. Chutia, S.I. Al-Resayes, S.K. Biswal, J. Mol. Struct. 1251 (2022) 132039.
[17] J.A. Obaleye, A.C. Tella, M.O. Bamigboye, Int. J. Med. Bio. Rech. 27 (2017) 24.
[18] Y. Wu, L. Hou, J. Lan, F. Yang, G. Huang, W. Liu, Y. Gou, J. Mol. Struct. 1279 (2023) 134986.
[19] C.A. Mcauliffe, J.V. Quagliano, L.M. Vallarino, Inorg. Chem. 5 (11) (1966) 1996–2003.
[20] M.K. Cristopher, K.E. Van Holde, A.G. Ahern, Biochemistry, 3rd ed., Benjamin Cummings, Sanfransisco, Calif, 2000.
[21] Metal complexes of amino acids and peptides 1 (1973) 121.
[22] I. Bertini, C. Luchinat, W. Maret, M. Zeppezauer (Eds.), Zinc enzymes, Birkhaused, Boston, 1986.
[24] I. Warad, M. Azam, S.I. Al-Resayes, M.S. Khan, P. Ahmad, M. Al-Nuri, S. Jodeh, A. Husein, S.F. Haddad, B. Hammouti, M. Al-Noaimi, Inorg. Chem. Commun 43 (2014) 155–161.
[25] M. Nazir, R. Khattak, M.S. Khan, I.I. Naqvi, Bull. Chem. Soc. Ethiop. 34 (3) (2020) 557–569.
[26] M. Azam, S.M. Wabaidurad, M. Alam, A. Trzesowska-Kruszynska, R. Kruszynski, S.I. Al-Resayes, F.F. Alqahtani, M.R. Khan, Rajendra, Polyhedron 195 (2021) 114991.
[27] S.I. Al-Resayes, M. Shakir, N. Shahid, M. Azam, A.U. Khan, Arab J. Chem. 9 (2016) 335–343.
[28] R.R. Sharp, L. Lohr, L. Miller, Prog Nucl Mag Res Sp. 38 (2001) 115–158.
[29] I.C. Ballhausen, Introduction to Ligand Field Theory, Longmans, Green and Co., New York, Toronto, London, 1962.
[30] A.B.P. Lever, Inorganic Electronic Spectroscopy, second ed., Elsevier, Amsterdam, 1984.
[31] S.S. Hassan, E.F. Mohamed, Appl. Organomet. Chem. 34 (2) (2020) e5258.
[32] M.M. El-ajaily, A.K. Sarangi, R.K. Mohapatra, S.S. Hassan, R. N. Eldaghare, P.K. Mohapatra, M.K. Raval, D. Das, A. Mahal, A. Cipurkovic, ChemistrySelect 4 (2019) 9999–10005.
[33] M. Gaber, S.K. Fathalla, H.A. El-Ghamry, Appld. Organomet. Chem. 33 (4) (2019) e4707.
[34] J. Padmanabhan, R. Parthasarathi, V. Subramanian, P. Chattaraj, J. Phys. Chem. A 111 (7) (2007) 1358–1361.
[35] F.M. Atlam, M.K. Awad, M. Gaber, S. Fathalla, Appl. Organomet. Chem. (2020) e5635.
[36] T.H. Al-Noor, R.K. Mohapatra, M. Azam, L.K.A. Karim, P.K. Mohapatra, A.A. Ibrahim, P.K. Parhi, G.C. Dash, M.M. El-ajaily, S.I. Al-Resayes, M.K. Raval, L. Pintilie, J. Mole. Struct. 1229 (2021) 129832.